PRELIMINARY STUDY ON SPACE-BORNE LASER ALTIMETER SUPPORTED AEROTRIANGULATION

YUE Chunyu[1] HE Hongyan[1] BAO Yunfei[1] XING Kun[1] and ZHOU Nan[1]
[1]Beijing Institute of Space Mechanics & Electricity, No. 104, Youyi Road, Haidian Distict, Beijing 100094, China,
Email: ycy1893@gmail.com

KEY WORDS: Satellite photogrammetry; space-borne laser altimeter; aerotriangulation; positioning accuracy

ABSTRACT: As a way of acquiring elevation with high accuracy and effectiveness, space-borne laser altimeter improves the 3-dimensional earth observation capability of satellite optical remote sensing imagery. And using high accuracy elevation observation of space-borne laser altimeter as control points accords with the trend of satellite photogrammetry without ground control points. The problems of satellite photogrammetry is firstly introduced, then the methods of space-borne laser altimeter supported aerotriangulation is described in this paper, which can solve these problems due to the characteristics of laser altimeter. The bundle adjustment error equations are established according to the earth observation of satellite image and space-borne laser altimeter, as well as the relationship of their exterior orientation elements. Elevation observations supplied by laser altimeter can be used as elevation control point to improve the accuracy of aerotriangulation, and the positioning accuracy is analyzed.

1. INTRODUCTION

Satellite photogrammetry stereoscopic surveying gets 3-Dimension information of the earth by aerotriangulation with satellite image matching. And the recent advance is satellite photogrammetry aerotriangulatio using as less control points as possible. As a way of acquiring elevation with high accuracy and effectiveness, laser altimeter improves the 3-dimensional earth observation capability of satellite optical remote sensing imagery. Therefore, space-borne laser altimeter supported satellite photogrammetry aerotriangulation can rise the elevation accuracy of DSM generated by satellite images with laser ranging as elevation control element. Addition, the laser altimeter observation data can be used as control points in satellite photogrammetry global surveying, when the geo-positing accuracy of space-borne laser altimeter is high enough.

Photogrammetry aerotriangulation adjusts the orientation elements of images and ground points coordinates in the same time by image geo-positioning model (collinear equation). And the image geo-positioning model precision should be high enough to get a good surveying accuracy. Ground control points are usually used to calibrate the orientation elements, and corresponding points in the overlap of images are matched to intersect ground point coordinates by the image geo-positioning model. However, there are some difficulties to be solved in photogrammetry aerotriangulation practice:

(1) It is difficult to set ground control points in some areas, for example, depopulated areas in western China.

(2) It is difficult to match corresponding points in some areas, such as desert areas or ocean areas. We can not find corresponding points automatically in texture repeat areas or texture indigence areas. The 3-Dimension information of these areas can not be obtained by intersection without corresponding points matching, either.

(3) Some areas' surfaces are not visible, such as vegetation cover areas or shadow areas. We can not obtain the 3-Dimension information of these areas intersection without corresponding points matching.

All the difficulties above can be well solved by combining the stereo mapping camera data and space-borne laser altimeter data.

(1) The laser altimeter observation data calculated to achieve high plane accuracy can be used as ground control points to avoid the human work of setting ground control points, which reduces the cost. And the laser altimeter observation data can be also used as global mapping ground control points.

Supported by National Natural Science Foundation of China under Grant 41401411, China 973 Program under Grant 61321001, and the High Resolution Earth Observation Special Fund under Grant GFZX040136.

Table 1 Comparison of elevation control point layout

Control points setting method	Accuracy	Amount	Distribution	Cost
Human	High	Small	Some areas none	High
Laser altimeter	High in some conditions	Large	Uniformity/wide	Low

(2) Space-borne laser altimeter acquires elevation by laser ranging the distance between satellite and ground point using the position and attitude of satellite without corresponding points matching.

(3) Laser can penetrate the vegetation cover, and the elevation of ground surface can be acquired by echo signal analysis of distinguishing ground surface data and non-ground surface data.

2. SPACE-BORNE LASER ALTIMETER SUPPORTED SATELLITE PHOTOGRAMMETRY SYSTEM

Four ground control points on the four corners and two columns elevation control points on two sides should be set of surveying block in photogrammetry aerial triangulation, as shown in Figure 1 (YUAN Xiuxiao, et al, 2004), in which the triangles are ground control points, and the black dots are elevation control points.

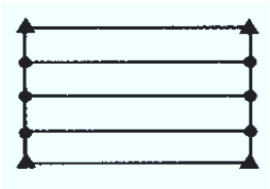

Figure 1 Control point in aerial triangulation

Plane and elevation accuracy of four IKONOS image aerial triangulation are 0.440m and 0.939m respectively, with four ground control points setting on the four corners of surveying block, which achieves the 1:10000 surveying accuracy (ZHANG Guo, et al, 2006). And the aerial triangulation accuracy is not rising with the number of ground control points rising. The conclusion is four ground control points on the four corners of surveying block is enough for surveying applications, which is very meaningful to satellite image aerial triangulation (ZHANG Guo, et al, 2006). ZY-3 image aerial triangulation plane and elevation accuracy are 2.93m and 2.07m respectively, with four GPS points as ground control points and fourteen GPS points as checking points, in which GPS points accuracy are higher than 0.1m (TANG Xinming, et al, 2012). Therefore, the high resolution remote sensing images can play a good performance in geo-positioning with only a few high accuracy ground control points on the proper position of the surveying block.

Two laser altimeters on the two sides of the stereo mapping camera beaming with a certain frequency, two columns of elevation control points are set on the two sides of image. Another plan is setting elevation control points, which are of distribution uniformity, by multibeam laser altimeter. The plans of space-borne laser altimeter supported aerotriangulation are shown in Figure 2, in which the black dots are footprints of space-borne laser altimeter.

(a) Laser footprint on two sides of image (b) Multibeam laser footprint

Figure 2 Laser footprint of space-borne laser altimeter supported aerotriangulation

The space-borne laser altimeter plane accuracy is not as high as its elevation accuracy, and the space-borne laser altimeter elevation accuracy is about tens of centimeters. The elevation and plane accuracy of the only space-borne laser altimeter for earth observation GLAS are 0.15m and tens of meters respectively (Sungkoo, et al, 2004). However, the elevation error propagation coefficients of space-borne laser altimeter angle exterior orientation elements are one several tenth of that of mapping camera (YU Junpeng and SUN Shijun, 2010). If the plane accuracy of space-borne laser altimeter is high enough by footprint calculation, laser altimeter can improve the elevation accuracy of earth

observation by aerotriangulation.

Satellite image photogrammetry geo-positioning function is Equation (1).

$$\begin{bmatrix} X_{\mathrm{P}} \\ Y_{\mathrm{P}} \\ Z_{\mathrm{P}} \end{bmatrix} = \begin{bmatrix} X_{\mathrm{SP}} \\ Y_{\mathrm{SP}} \\ Z_{\mathrm{SP}} \end{bmatrix} + \lambda \begin{bmatrix} a_{1\mathrm{P}} & a_{2\mathrm{P}} & a_{3\mathrm{P}} \\ b_{1\mathrm{P}} & b_{2\mathrm{P}} & b_{3\mathrm{P}} \\ c_{1\mathrm{P}} & c_{2\mathrm{P}} & c_{3\mathrm{P}} \end{bmatrix} \begin{bmatrix} x \\ y \\ -f \end{bmatrix} \tag{1}$$

Space-borne laser altimeter geo-positioning function is Equation (2).

$$\begin{bmatrix} X_{\mathrm{L}} \\ Y_{\mathrm{L}} \\ Z_{\mathrm{L}} \end{bmatrix} = \begin{bmatrix} X_{\mathrm{SL}} \\ Y_{\mathrm{SL}} \\ Z_{\mathrm{SL}} \end{bmatrix} - L \begin{bmatrix} a_{1\mathrm{L}} & a_{2\mathrm{L}} & a_{3\mathrm{L}} \\ b_{1\mathrm{L}} & b_{2\mathrm{L}} & b_{3\mathrm{L}} \\ c_{1\mathrm{L}} & c_{2\mathrm{L}} & c_{3\mathrm{L}} \end{bmatrix} \begin{bmatrix} 0 \\ \sin\theta \\ \cos\theta \end{bmatrix} \tag{2}$$

$(X_{\mathrm{P}}, Y_{\mathrm{P}}, Z_{\mathrm{P}})$ and $(X_{\mathrm{L}}, Y_{\mathrm{L}}, Z_{\mathrm{L}})$ are the ground coordinates acquired by mapping camera and space-borne laser altimeter respectively, (X_{SP}, Y_{SP}, Z_{SP}) and (X_{SL}, Y_{SL}, Z_{SL}) are the line exterior orientation elements, $(a_{1\mathrm{P}}, a_{2\mathrm{P}}, a_{3\mathrm{P}}, b_{1\mathrm{P}}, b_{2\mathrm{P}}, b_{3\mathrm{P}}, c_{1\mathrm{P}}, c_{2\mathrm{P}}, c_{3\mathrm{P}})$ and $(a_{1\mathrm{L}}, a_{2\mathrm{L}}, a_{3\mathrm{L}}, b_{1\mathrm{L}}, b_{2\mathrm{L}}, b_{3\mathrm{L}}, c_{1\mathrm{L}}, c_{2\mathrm{L}}, c_{3\mathrm{L}})$ are the direction cosine functions of angle exterior orientation elements, $(x, y, -f)$ are the interior orientation elements of mapping camera, λ is mapping scale, L is the laser ranging value, θ is the pointing angle of laser altimeter.

The space-borne laser altimeter supported bundle aerotriangulation adjustment error equations are composed by the ground coordinates and orientation elements measurement values of space-borne laser altimeter and mapping camera without ground control points are in Equation (3).

$$\left.\begin{array}{ll} V = A_1 t_1 + B_1 x_1 - l & P \\ V_{\mathrm{las}} = A_2 t_2 + B_2 x_2 - l_{\mathrm{las}} & P_{\mathrm{las}} \\ V_{\mathrm{C}} = C x_3 - l_{\mathrm{C}} & P_{\mathrm{C}} \\ V_{t_1} = t_1 & P_{t_1} \\ V_{t_2} = t_2 & P_{t_2} \end{array}\right\} \tag{3}$$

The first function in Equation (3) is observation error equation of stereo mapping camera image point coordinates, the second function in Equation (3) is observation error equation of space-borne laser altimeter ranging, the third function in Equation (3) is observation error equation of the exterior orientation elements relationship between stereo mapping camera and space-borne laser altimeter, the fourth function in Equation (3) is observation error equation of the stereo mapping camera exterior orientation elements, and the fifth function in Equation (3) is observation error equation of the space-borne laser altimeter exterior orientation elements. V, V_{las}, V_{C}, V_{t_1}, and V_{t_2} are the observation correction vectors. t_1 and t_2 are exterior orientation element vector of stereo mapping camera and space-borne laser altimeter respectively. x_1 and x_2 are geo-positioning coordinate vectors of stereo mapping camera and space-borne laser altimeter. x_3 is the observation vector of relationship between stereo mapping camera exterior orientation elements and space-borne laser altimeter exterior orientation elements. A_1, A_2, B_1, B_2, and C are coefficients matrix. l, l_{las}, and l_{C} are observation residual errors. P, P_{las}, P_C, P_{t_1}, and P_{t_2} are the observations weights of each error equation.

3. EXPERIMENTS AND ANALYSIS

3.1 Space-borne Laser Altimeter Geo-positioning

The space-borne laser altimeter geo-positioning is shown in Figure 3. S is the position of space-borne laser altimeter, P is the ground point, L is the laser ranging value, θ is the pointing angle of laser altimeter, (*φ, ω, κ*) are angle

exterior orientation elements.

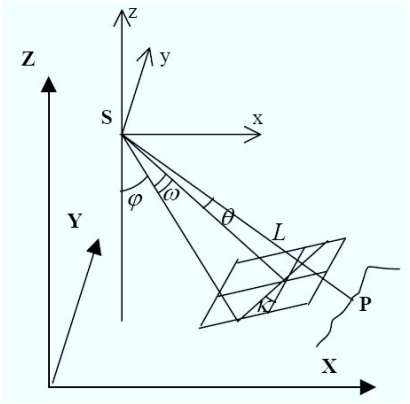

Figure 3 Geometric position of space-borne laser altimeter

Equation (2) is linear expansion by Talor expansion method. as Equation (4).

$$\begin{bmatrix} X \\ Y \\ Z \end{bmatrix} = \begin{bmatrix} X_0 \\ Y_0 \\ Z_0 \end{bmatrix} + \begin{bmatrix} \frac{\partial X_0}{\partial X_{S0}} & \frac{\partial X_0}{\partial Y_{S0}} & \frac{\partial X_0}{\partial Z_{S0}} & \frac{\partial X_0}{\partial \varphi_0} & \frac{\partial X_0}{\partial \omega_0} & \frac{\partial X_0}{\partial \kappa_0} & \frac{\partial X_0}{\partial L_0} & \frac{\partial X_0}{\partial \theta_0} \\ \frac{\partial Y_0}{\partial X_{S0}} & \frac{\partial Y_0}{\partial Y_{S0}} & \frac{\partial Y_0}{\partial Z_{S0}} & \frac{\partial Y_0}{\partial \varphi_0} & \frac{\partial Y_0}{\partial \omega_0} & \frac{\partial Y_0}{\partial \kappa_0} & \frac{\partial Y_0}{\partial L_0} & \frac{\partial Y_0}{\partial \theta_0} \\ \frac{\partial Z_0}{\partial X_{S0}} & \frac{\partial Z_0}{\partial Y_{S0}} & \frac{\partial Z_0}{\partial Z_{S0}} & \frac{\partial Z_0}{\partial \varphi_0} & \frac{\partial Z_0}{\partial \omega_0} & \frac{\partial Z_0}{\partial \kappa_0} & \frac{\partial Z_0}{\partial L_0} & \frac{\partial Z_0}{\partial \theta_0} \end{bmatrix} \begin{bmatrix} \Delta X_S \\ \Delta Y_S \\ \Delta Z_S \\ \Delta\varphi \\ \Delta\omega \\ \Delta\kappa \\ \Delta L \\ \Delta\theta \end{bmatrix} \tag{4}$$

(X, Y, Z) are the coordinates of P, (X_S, Y_S, Z_S) are the line exterior orientation elements of space-borne laser altimeter, (X_0, Y_0, Z_0) are the observations of (X, Y, Z), （X_{S0}, Y_{S0}, Z_{S0}, φ_0, ω_0, κ_0） are the initial values of exterior orientation elements, (ΔX_S, ΔY_S, ΔZ_S, $\Delta\varphi$, $\Delta\omega$, $\Delta\kappa$, ΔL, $\Delta\theta$） are the errors. The accuracy of (X, Y, Z) in Equation (4) is as below.

$$\begin{bmatrix} \delta_X \\ \delta_Y \\ \delta_Z \end{bmatrix} = \begin{bmatrix} \sqrt{\left(\frac{\partial X}{\partial X_S}\right)^2 (\Delta X_S)^2 + \left(\frac{\partial X}{\partial Y_S}\right)^2 (\Delta Y_S)^2 + \left(\frac{\partial X}{\partial Z_S}\right)^2 (\Delta Z_S)^2 + \left(\frac{\partial X}{\partial \varphi}\right)^2 (\Delta\varphi)^2 + \left(\frac{\partial X}{\partial \omega}\right)^2 (\Delta\omega)^2 + \left(\frac{\partial X}{\partial \kappa}\right)^2 (\Delta\kappa)^2 + \left(\frac{\partial X}{\partial L}\right)^2 (\Delta L)^2 + \left(\frac{\partial X}{\partial \theta}\right)^2 (\Delta\theta)^2} \\ \sqrt{\left(\frac{\partial Y}{\partial X_S}\right)^2 (\Delta X_S)^2 + \left(\frac{\partial Y}{\partial Y_S}\right)^2 (\Delta Y_S)^2 + \left(\frac{\partial Y}{\partial Z_S}\right)^2 (\Delta Z_S)^2 + \left(\frac{\partial Y}{\partial \varphi}\right)^2 (\Delta\varphi)^2 + \left(\frac{\partial Y}{\partial \omega}\right)^2 (\Delta\omega)^2 + \left(\frac{\partial Y}{\partial \kappa}\right)^2 (\Delta\kappa)^2 + \left(\frac{\partial Y}{\partial L}\right)^2 (\Delta L)^2 + \left(\frac{\partial Y}{\partial \theta}\right)^2 (\Delta\theta)^2} \\ \sqrt{\left(\frac{\partial Z}{\partial X_S}\right)^2 (\Delta X_S)^2 + \left(\frac{\partial Z}{\partial Y_S}\right)^2 (\Delta Y_S)^2 + \left(\frac{\partial Z}{\partial Z_S}\right)^2 (\Delta Z_S)^2 + \left(\frac{\partial Z}{\partial \varphi}\right)^2 (\Delta\varphi)^2 + \left(\frac{\partial Z}{\partial \omega}\right)^2 (\Delta\omega)^2 + \left(\frac{\partial Z}{\partial \kappa}\right)^2 (\Delta\kappa)^2 + \left(\frac{\partial Z}{\partial L}\right)^2 (\Delta L)^2 + \left(\frac{\partial Z}{\partial \theta}\right)^2 (\Delta\theta)^2} \end{bmatrix}$$

(4)

The line exterior orientation elements accuracy of recent high resolution remote sensing satellite is tens of centimeters (YU Junpeng, et al, 2011), while the angle exterior orientation elements accuracy is higher than 1″. Just take the flat areas as consideration. Make an assumption that, the pointing angle of laser altimeter error is 1″, the ranging error is 0.3m, which includes hydrostatic delay, earth tide, and footprint, etc, according to GLAS (FAN Chunbo, et al, 2007). Assume the ranging value L=500km, which is equal to the orbital altitude, $\varphi = \omega = \kappa \approx 0$, the laser altimeter pointing to the satellite ground track, $\theta=0$. So in Equation(5), $\Delta X_S=\Delta Y_S=\Delta Z_S$=0.1m, $\Delta\varphi=\Delta\omega=\Delta\kappa=\Delta\theta$=1″, ΔL=0.3m. We can get δ_X=2.43m, δ_Y=2.43m, δ_Z=0.32m in Equation(5). When the resolution of remote sensing image is lower than 5m, the plane accuracy of laser altimeter is within one pixel, and can be ignored.

3.2 Simulation Space-borne Laser Altimeter Supported Aerotriangulation

The simulation space-borne laser altimeter observations are combined with real satellite remote sensing images, and space-borne laser altimeter supported bundle aerotriangulation adjustment with Equation (3) is processed to analyze the geo-positioning accuracy. The space-borne laser altimeter geo-positioning accuracy is the same as 3.1, δ_X=2.43m, δ_Y=2.43m, δ_Z=0.32m. The second row of Tab. 2 is the original accuracy of satellite remote sensing image. As the

beaming frequency of space-borne laser altimeter is low, it is difficult to get a lot of ranging observations in the surveying block, and we just set four laser altimeter observations on the four corners of the image. The experiment results is shown in Tab. 2, and the third row is the laser altimeter supported aerotriangulation accuracy.

Tab.2 Experiment result

Accuracy	*X*	*Y*	Plane	*Z*
Original	45.15 m	52.38 m	69.15 m	16.63 m
Laser altimeter supported aerotriangulation	2.56 m	3.30 m	4.18 m	8.95 m

The laser altimeter supported aerotriangulation accuracy is higher with the assumption of 3.1, which can be seen from Table 2.

4 CONCLUSION

The method and necessary of space-borne laser altimeter supported aerotriangulation are described in this paper. And the plan of space-borne laser altimeter supported aerotriangulation is proposed according to the experiences and principles of photogrammetry aerotriangulation practice. The experiments of space-borne laser altimeter geo-positioning accuracy and simulation space-borne laser altimeter supported aerotriangulation are taken. The earth observation accuracy can be improved by space-borne laser altimeter supported aerotriangulation. However, the footprint, whose shape is changing with the terrain, is a big error souse of space-borne laser altimeter geo-positioning. The follow research should be focused on the geometrical calibration or footprint geolocation of space-borne laser altimeter to improve the plane accuracy, which is very necessary to the earth observation.

REFERENCES

FAN Chunbo, et al, 2007. ICEsat/GLAS Laser Footprint Geolocation and Error Analysis. Journal of Geodesy and Geodynamic, 27 (1), pp. 104-106.

Sungkoo Bae, et al, 2004. Charles Web, and Bob Schutz. GLAS PAD Calibration Using Laser Reference Sensor Data. In: AIAA/AAS Astrodynamics Specialist Conference and Exhibit, Providence, RI, USA, pp. 1-10.

TANG Xinming, et al, 2012. Triple Linear-array Imaging Geometry Model of ZY-3 Mapping Satellite and Its Validation. Acta Geodaeticaet Cartographica Sinica, 41 (2), pp. 191-198.

YUAN Xiuxiao, et al, 2004. GPS-supported bundle block adjustment without ground control Points. Geomatics and Information Science of Wuhan University, 29 (10), pp. 852-857.

YU Junpeng and SUN Shijun, 2010. Some Strategies about Satellite Photogrammetry. In: The 23rd National conference on space explorer, Xiamen, China, pp. 1-6.

YU Junpeng, et al, 2011. Study on Error Propagation of Exterior Orientation Elements of Satellite Remote Sensing Imagery. Spacecraft Recovery & Remete Sensing, 32 (1), pp. 18-23.

ZHANG Guo, et al, 2006. The Mapping Accuracy of Satellite Imagery Block Adjustment. Journal of Zhengzhou Institute of Surveying and Mapping, 23(4), pp. 239-241.